

[5] Dynamic analysis of optical cell trapping in the ray optics regime



S.S. Klykov¹, I.V. Fedosov¹, V.V. Tuchin^{1,2,3}

¹N.G. Chernyshevskiy Saratov State University, Saratov, Russia

²Institute of Precision Mechanics and Control of Russian Academy of Sciences, Saratov, Russia

³Tomsk State University, Tomsk, Russia

Abstract

We analyze forces that act in an optical trap on a biological cell modeled by a dielectric microsphere moving in a fluid. Analysis of the microsphere's dynamical behavior has enabled key parameters for trapping of the cell to be identified, including the fluid viscosity and the laser beam power.

Keywords: OPTICAL TWEEZERS, OPTICAL CONFINEMENT AND MANIPULATION, LASER TRAPPING, RAY OPTICS MODEL OF OPTICAL TRAP

Citation: KLYKOV S.S. DYNAMIC ANALYSIS OF OPTICAL CELL TRAPPING IN THE RAY OPTICS REGIME //

COMPUTER OPTICS. – 2015. – Vol. 39(5). – P. 694-701.

Introduction

To measure forces which act in optical blood cell trapping in capillaries *in vivo*, it is necessary to use good calibration methods for trap stiffness [1,2]. For the time being, the most widely used calibration methods can't be applied under *in vivo* trapping conditions, since these methods basically suggest both controlled influence on a particle, and tracking a particle position by means of a photodetector (Quadrant Photo Detector – QPD) using scattered light by particle [3]. The evaluation of trap stiffness under *in vivo* conditions may be performed using video microscopy tracking of spatial position of a cell [4] and also by means of further analysis of its dynamics in trapping [1,5]. To construct a dynamic model of cell trapping, it is necessary to analyze in detail the forces which act on the cell in optical cell trapping.

There are three classes of objects identified, for which various calculation methods for the forces acting in optical trapping have been developed, i.e. small particles with a diameter less than 0.1λ (Rayleigh approximation), particles with intermediate dimensions from 0.1λ to 10λ and large particles with the diameter more than 10λ (ray optics approximation) [6]. Thus, red blood cells have geometrical dimensions which allow us to consider the problem of their optical trapping in the ray optics regime [7,8]. To simplify the calculations, we may consider (as an elementary model of a cell) a microsphere with proper geometrical dimensions [1,9].

The classical theory for calculating the forces in the ray optics approximation has been developed in papers [10,11], and this theory is now widely used for numeric evaluations of parameters of various experiments and for the construction of their mathematical models [12-16]. This paper proposes a dynamic trapping model for microspheres with the dimensions $d \geq 10\lambda$, when they move through a wide capillary at a constant speed. Based on this model, we have considered the microsphere trapping conditions depending on the motion speed, the focused laser radiation power and the dynamic fluid viscosity. It was found out that the maximum speed at which the trapping is possible may be determined by the fluid viscosity and the beam power. Therefore, at proper power and speed values, we may determine the local fluid viscosity in which microspheres or cells move around. In the absence of trapping (at a sufficiently high motion speed) the analysis of time dependence of a microsphere centre coordinate on the radiation power in a focused beam will be performed. This analysis may be used when calibrating trap stiffness under the optical trapping conditions *in vivo*.

To develop the dynamic trapping model, we have derived the calculating formulas of spatial dependence of the acting force based on the analysis of geometrical shifts of photon momentum [17]. This approach enabled to analyze the refraction of beams belonging to different quadrants of microscope objective aperture, and also to get explicitly a calculating formula of

the force dependence on the distance between the microsphere center and a beam focus. It is worth to note that the calculating formulas of the classical theory have been formally developed for the case of loosely focused beams (i.e. for a focusing lens with a small numerical aperture) [10,18]. Therefore, dividing the net optical force, which acts on the microsphere, into the gradient force and the scattering force performed for the focused beam [11] was not formally justified. So, in this paper based on the analysis of beam refraction, we have derived the expression coinciding with that one earlier obtained [11] for the force which can be interpreted as the gradient force.

1. Geometrical model of an optical trap

To derive the calculating formulas for the forces which act on an object in the optical trap, let's consider refraction of the focused beam by microsphere. When the direction of beam propagation changes, photon momentums directed along the beam vary. Variation of momentum may be caused only by the effective force acting from the microsphere. Therefore, according to the Newton's third law, the microsphere is acted by the opposite force which can be written as follows: [11]:

$$F = Q \frac{nP}{c} \quad (1)$$

where Q – is the dimensionless coefficient, n – is the refractive index of a medium encircling the microsphere, P – is the radiation power of the focused beam, the focus size of which is much less than the microsphere geometrical sizes, c – is the speed of light in vacuum.

Thus, to calculate the force acting on the object in the trap, it is necessary to calculate the dimensionless coefficient Q , which depends on geometrical changing the linear momentum of photons due to beam refraction and reflection on the surface of the dielectric microsphere.

In classical papers [10,11] the force acting on the microsphere was divided into two components: the scattering force (F_s) and the gradient force (F_G). For each of these forces we have introduced the following respective geometric factors q_s and q_G , which may be referred to the single-beam refraction [11]:

$$q_s = 1 + R \cos 2\theta - \frac{T^2 [\cos(2\theta - 2\theta') + R \cos 2\theta]}{1 + R^2 + 2R \cos 2\theta'} \quad (2)$$

$$q_G = R \sin 2\theta - \frac{T^2 [\sin(2\theta - 2\theta') + R \sin 2\theta]}{1 + R^2 + 2R \cos 2\theta'} \quad (3)$$

The variables contained in the above expressions (2) and (3) will be clarified below.

Refraction by microsphere is considered further at the following approximations:

1. The focused beam is considered to be stigmatic, however aberrations existing when focusing are not taken into account (the degree of impact of aberrations onto experimentally trap-measured forces has been set out in paper [19]).

2. Geometrical size of a focal spot is considered to be negligibly small compared to object dimensions, provided it's true for lenses with large numeric apertures used for optical trapping.

We have treated as a microsphere material both polystyrene (PS) with the refraction index $n_s = 1.57$ and isotropic dielectric with the refraction index 1.4 equal to the refraction index of a red blood cell [20]. As a medium in which microspheres moved, we have considered blood plasma and distilled water with the refraction index which is close to the refraction index of blood plasma $n_w = 1.33$ [20], but its dynamic viscosity differs from the first medium. The selection of polystyrene as the microsphere material is explained by two reasons: firstly, this material is discussed in classical paper [11] in order to calculate values of the dimensionless coefficient Q ; therefore, this option is convenient to compare calculation results. Secondly, polystyrene microspheres are convenient objects for the implementation of algorithms of video microscopy tracking in optical trapping [2,4]. The difference in refraction indices between polystyrene (1.57) and red blood cells (1.4) [20] during calculations results in decreasing the effective force, which may be compensated by increasing the laser radiation power to an appropriate value. The value of this power compensation is averagely 2.8 times. Notice that the considering wavelength of laser radiation λ belongs to the near infrared (IR) region in which radiation absorption by red blood cells and polystyrene is small.

Let's construct a decomposition diagram (Fig. 1) of aperture microlens by quadrants to which microsphere-refracted beams belong, because the momentum changing projections after the refraction of beams belonging to different quadrants are different [21].

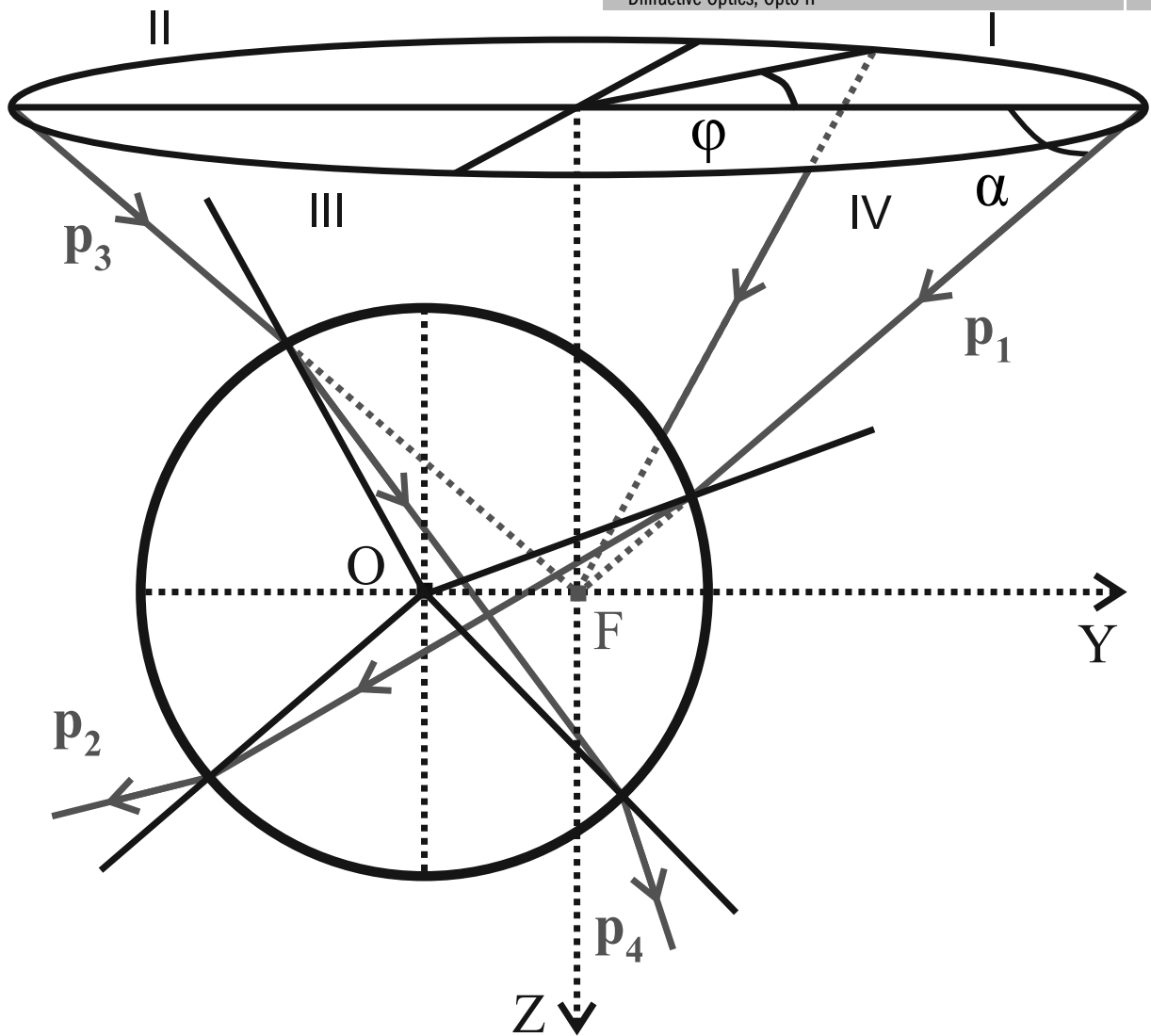


Fig.1. Microsphere refraction of beams belonging to different quadrants

Fig. 1 introduces the following notations: p. O – is the microsphere center, p. F – is the beam focus (trap center), OZ-axis – is the direction of beam propagation, OY-axis – is the direction of microsphere motion, the angles α and ϕ – are the angles which set a position of the incident beam with respect to objective aperture. As observed in Fig.1, OY-axis projections of photon momentums belonging to the refracted beams depend on beam inhering to one of the following quadrant pairs: I/IV and II/III. This may explain a particular impact of refracted beams onto the resulting momentum change.

It necessary to construct a refraction scheme for the beam belonging to quadrant I (Fig. 2) and analyze the change of the direction of its propagation after its refraction for further deriving of explicit equations.

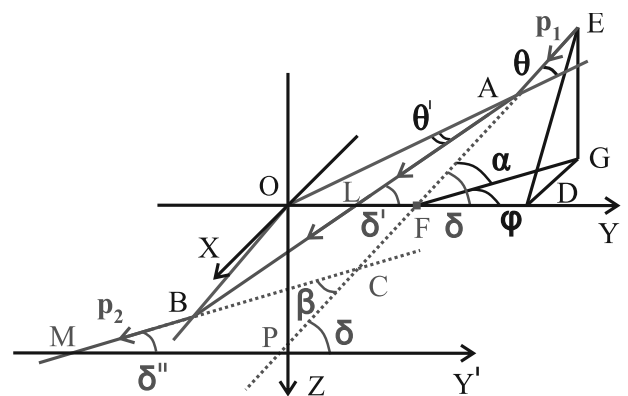


Fig.2. Refraction scheme for the beam belonging to quadrant I

So let's clarify some notations in Fig.2: the angle θ – is the beam incidence angle, the angle θ' – is the refraction angle, OA, OB – are the normal lines to the sphere

surface, OX-axis is perpendicular to OZ- and OY-axes. The direction of the incident beam is defined by vector \mathbf{p}_1 , and of the refracted beam at the sphere exit – by \mathbf{p}_2 , EG – is a perpendicular to OXY-plane. Then the angle δ formed by the incidence beam and the straight line OY may be determined from the following condition: $\cos \delta = \cos \alpha \cos \varphi$

From the triangle OAF, in which lateral lengths are equal, we have the following: $OA=R$ – is the microsphere radius, $OF=S$ – is the distance between microsphere and trap centers according to the sine theorem: $\sin \theta = \frac{S}{R} \sin \delta$.

In particular, this relationship defines a dramatic drop in the gradient force at distances which are larger than the radius R , because the beams with the largest incidence angle cease to be refracted by the microsphere and, consequently, to contribute to the resulting momentum change.

From the triangle LAF we have $\delta' = \delta - \theta + \theta'$. From the triangle ACB we have $\beta = 2(\theta - \theta')$

Let's draw an additional axis $O'Y' \uparrow \uparrow OY$, and from the constructed triangle CPM we have $\delta'' = \delta - \beta$. Due to these arrangements the projection p_2 onto the axis OY is as follows: $p_{2Y} = -T(\theta)^2 \cos(\delta - \beta)$, where $T(\theta)$ – is the Fresnel transmission coefficient.

Then, the momentum change along the axis OY for quadrant I is written as follows:

$$\Delta p'_{Y} = p_{2Y} - p_{1Y} = -\left(T(\theta)^2 \cos(\delta - \beta) - \cos \delta\right) \quad (4)$$

Thus, the momentum change is $\Delta p'_{Y} < 0$, and it is directed into the sphere center, therefore $F_{Y'} > 0$, i.e. $F_{Y'}$ may be interpreted as the gradient force which attempts to get back the sphere to the equilibrium position, where the focus coincides with the sphere center.

The momentum change expression (4) takes into account the fact that the refracted beam momentum has been decreased due to reflection from two interface borders, i.e. fluid-microsphere and microsphere-fluid, through multiplying by the transmission coefficient $T(\theta)$

Construction of the refraction scheme for the beam which belongs to quadrant II may be performed similarly to the aforementioned scheme with regard to the angle mirror symmetry.

Keeping the geometrical meaning of notations for projection angles of the beam momentum change from quadrant II, there can be obtained the following equation:

$$\Delta p''_{Y} = p_{2Y} - p_{1Y} = T(\theta)^2 \cos(\delta + \beta) - \cos \delta \quad (5)$$

Thus, the momentum change depends on the beam inhering to one of the quadrant pairs. The momentum change, which occurs due to the beam

reflection, should be mutually compensated for mirror-symmetrical beams. Therefore, the beam momentum change is not equal for all quadrants, as mentioned in paper [11].

Further, let's sum in modulus the expressions (4) and (5) and convert them to a final expression which describes the momentum projection change to the axis OY as follows:

$$\Delta p_Y = T(\theta)^2 \sin \delta \sin \beta \quad (6)$$

The formula expressing the spatial dependence of the coefficient Q included into the expression (1) and defining the effective force is as follows:

$$Q_Y(S) = k \int_0^{\pi/2} \int_{\pi/9}^{\pi/2} \Delta p_Y(\alpha, \varphi, S) d\alpha d\varphi, \quad (7)$$

where k – is the normalizing coefficient equal to $\frac{1}{\pi}$.

This coefficient has been selected with regard to the equation of maximum calculating coefficients according to the above formula (7) with the values given in paper [11].

The previously derived formula [11] for calculation of the gradient force $F_G = q_G \sin \delta$ relating to the single-beam refraction coincides with the formulas derived in this paper to change the momentum Δp_Y , if we set equal the Fresnel transmission coefficient $R \rightarrow 0$. As noted above, we can't take into account the refracted beams regardless of the beam inhering to one of the quadrants.

A lower integration limit in the above formula (7) by the aperture angle α has been selected as equal to the value used in paper [11]. This limiting angle conforms with immerse lenses with the numeric apertures more than 1.2 ($NA \geq 1.2$), which are to be implemented in practice for 3D-trapping of various microparticles [3,13] cells included [1,2].

2. Dynamics analysis of optical cell trapping

Dynamic analysis of optical cell trapping is based on the following model: the microsphere (as a cell model [1,5]) moves on flowing in fluid through a channel at a constant speed V_o , so that its center is on the same axis as the beam focus (OY-axis). The considered dynamics of optical cell trapping in the plane, where there is the beam focus, may be explained by the fact that in 3D-trapping on this plane the lateral component F_z of the gradient force acting on a microparticle is actually equal to zero, that allows us to analyze a trapping problem only on the transverse plane OXY. If the axial force is sufficient for trapping, then during this process the particle will move along the axis OZ, until it reaches an equilibrium point which lies near the focus that will not influ-

ence on possible trapping in the transverse plane. The similar breaking of a 3D-trapping problem into subproblems which consider the acting forces in two perpendicular planes was performed in most of subject-mattered papers, for example, in [1,10,11,17,18]. Furthermore, it is meaningless to consider the dynamics of cells moving out-of-focus, because it is impossible to provide video microscopy tracking of their dynamics, and therefore, to perform experimental calibration of trap stiffness, one of the methods of which has been analyzed herein.

The force dependence

$$F_y(S) = \frac{nP}{c} Q_y(S)$$

is determined according to the above formulas (1) and (7). The speed, at which the trapped microsphere is drawn from the trap thereafter, is still determined by this restoring force. Therefore, this speed is approximately 100 $\mu\text{m/s}$, when the incident power is 10 mW. Based on this relationship, one of the classical methods for measuring trap stiffness, i.e. the “drag force method” [3], is based.

The motion equation has a standard writing in accordance with to the Newton’s second law [22]:

$$m \frac{dV(S)}{dt} = F_y(S) + \gamma(V_0 - V(S)), \quad (8)$$

where $\gamma = 6\pi\eta r$ – is the Stokes’s drag coefficient for the sphere.

The equation (8) does not take into account the Langevin random force which characterizes the Brownian motion [22] of the particle, because the Brownian motion of fluid particles with dimensions of 10 μm max is sufficiently small.

The calculation results are given below in Fig. 3a.-3d., which were calculated at various values of the incident power P, different original motion speeds of the microsphere V_0 , and the dynamic fluid viscosity η . The above mentioned parameters define in total the possibility of optical microsphere trapping. The microsphere radius is supposed to be equal to 5 μm . We consider the microsphere optical trapping on flowing in water and blood plasma with proper dynamic viscosity values: for water – 10^{-3} Pa·s [22] and for blood plasma – $1.2 \cdot 10^{-3}$ Pa·s [1]. Edge effects connected with the motion near the channel walls are not considered herein (it is assumed that the channel is wide enough), therefore the viscosity values are assumed equal to the tabulated values.

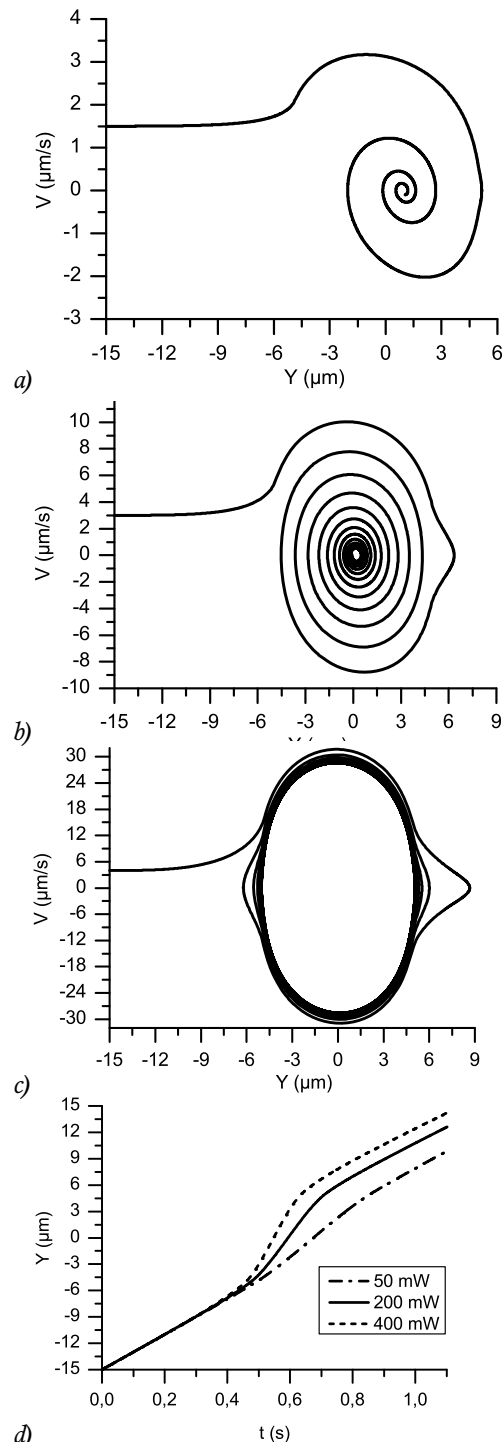


Fig.3. Trajectories of trapped microspheres with $n_s = 1.57$ under different conditions: a – is a phase trajectory on moving in water flow at the value of the incident power 1 mW; b – at the value of the incident power 10 mW; c – at the value of the incident power 100 mW; d – is the dynamics of changing the microsphere center coordinate on flowing in blood plasma at different values of the incident power and at the value of the original speed equaled to 20 $\mu\text{m/s}$

The critical maximum speed, at which it is still possible to provide microsphere trapping, goes up rather slowly as the trap radiant power significantly increases (from 1.6 $\mu\text{m/s}$ at 1 mW to 7.2 $\mu\text{m/s}$ at 100 mW – the values are given in the table below). The power increase results in changing the phase trajectory due to a small viscosity coefficient compared to acceleration and speed values achieved at microsphere trapping. Thus, the parameter defining the critical speed is the dynamic viscosity of the medium in which cells move. This dependence may be accepted as a basis for a new noninvasive fluid viscosity method. This method may be based both on cell-motion tracking at different powers and the constant speed, and on tracing the trapping effect at a constant power and a varying cell-motion speed.

Table. Values of maximum speeds

	1 mW	10 mW	100 mW
For the flowing microsphere with $n_s = 1.57$ in water	1.6 $\mu\text{m/s}$	3.6 $\mu\text{m/s}$	7.2 $\mu\text{m/s}$
For the flowing microsphere with $n_s = 1.57$ in blood plasma	1.7 $\mu\text{m/s}$	3.8 $\mu\text{m/s}$	7.8 $\mu\text{m/s}$
For the flowing microsphere with $n_s = 1.4$ in blood plasma	1.2 $\mu\text{m/s}$	2.9 $\mu\text{m/s}$	6.3 $\mu\text{m/s}$

Given the dependence of capillary walls on slowing down the cells (for example, based on the Faxen's law [23]), it becomes possible to provide cell trapping on capillary flowing. Therefore, in order to reduce the required power for permanent cell trapping *in vivo*, it is necessary to place a trap center close to a capillary wall.

Fig. 3d gives the dynamic characteristic of the coordinate $y(t)$ when the microsphere passes through the trap. From Fig. 3 it is seen that the more the incident power, the more a deviation from the rectilinear law of the coordinate variation of the microsphere center by trapping. The cell trajectory distortion in capillaries may supplement the existing methods of trap stiffness calibration *in vivo* [1,5]. Note that the

bend-tracing process under experimental conditions may be rather difficult. Nevertheless, the trap stiffness or the existing force may be evaluated by the coordinate time-dependent displacement at a constant motion speed.

3. Results and discussion

This paper considers the dynamic analysis of optical trapping for the microsphere with the diameter of 10 μm , when it moves in fluid at a constant speed rate. To construct a numerical model of the trapping dynamics, we have explicitly derived a formula required to calculate the dependence of forces, which act on the microsphere in the trap, on the distance between the microsphere center and the beam focus. This approach was based on the geometric calculation of photon momentum variations when refracting on microsphere surfaces.

Furthermore, we have analyzed in this paper some trapping conditions for the microsphere at its axial movement with respect to the trap center. We have calculated maximum speed rates at which it was possible to provide trapping of the microsphere depending on the incident power, the dynamic viscosity of the fluid and the microsphere material. This dependence seemed to be non-proportional for different materials: when the incident power was changed tenfold, the critical speed was increased approximately twofold (see the above Table). Therefore, for the successful cell trapping *in vivo*, it is necessary to arrange the optical trap close to capillary walls in order to create the additional friction effect acting from walls to the cell. The above mentioned effect may also be applied on non-axial cell motions with respect to the trap center. In this case only the cell motion trajectory significantly differs from the axial movement considered herein.

The dynamics of the microsphere motion in the trap and the possibility of trapping is determined not only by the beam radiation power, but also by the fluid viscosity (Fig. 3.a. – 3.c.). This fact may be taken as a basis for a new method to determine the local viscosity of blood plasma that would enable to expand application areas of optical manipulation performed *in vivo* [1,2]. In the absence of trapping, the optical trap provokes the microsphere motion distortion on flowing in fluid and, respectively, changing the dependence of the microsphere center position y on the time t . The value of this distortion de-

pend, first of all, on the original speed and the incident power that might be used to develop a new calibration method for trap stiffness applied for trapping *in vivo* [1-3,5].

To discuss in detail the dynamics of optical cell trapping, it is necessary to analyze the force spatial dependence for a refracting object which has a shape corresponding to the blood cell.

Acknowledgements

This work is supported by competitive contract № 3.1340.2014/K of The RF Ministry of Science and Education, by research and development RF government contract № 2014/203, Research № 1490 “Development of optical methods and instrumentation for measurements and control of structure and dynamics of biological media”, and by grant of The President of RF NSh-703.2014.2

References

1. Zhong M.-C., Wei X.-B., Zhou J.-H., Wang Z.-Q., Li Y.-M. Trapping red blood cells in living animals using optical tweezers. *Nature Communications* 2013; 4(1768): 1-7. DOI: 10.1038/ncomms2786
2. Zhong M.-C., Gong L., Zhou J.-H., Wang Z.-Q., Li Y.-M. Optical trapping of red blood cells in living animals with a water immersion objective. *Optics Letters* 2013; 38(23): 5134-37. DOI: 10.1364/OL.38.005134
3. Sarshar M., Wong W.T., Anvari B. Comparative study of methods to calibrate the stiffness of a single-beam gradient-force optical tweezers over various laser trapping powers. *J. Biomed. Opt.* 2014; 19(11): 115001-1 – 115001-13. DOI: 10.1117/1.JBO.19.11.115001
4. McAlinden N., Glass D.G., Millington O.R., Wright A.J. Accurate position tracking of optically trapped live cells. *Biomed. Opt. Express* 2014; 5(4): 1026-1037. DOI: 10.1364/BOE.5.001026
5. Wu Y., Sun D., Huang W., Xi N. Dynamics analysis and motion planning for automated cell transportation with optical tweezers. *IEEE/ASME Trans. Mech.* 2013; 18(2): 706-713. DOI: 10.1109/TMECH.2011.2181856
6. Nieminen T.A., Preez-Wilkinson N., Stilgoe A.B., Loke V.L.Y., Bui A.A.M., Rubinsztein-Dunlop H. Optical tweezers: Theory and modeling. *J. Quant. Spect. & Rad. Trans.* 2014; 146: 59-80. DOI: 10.1016/j.jqsrt.2014.04.003
7. Sraj I., Sztatmary A.C., Marr D.W.M., Eggleton C.D. Dynamic ray tracing for modeling optical cell manipulation. *Optics Express* 2010; 18(16): 16702-16714. DOI: 10.1364/OE.18.016702
8. Hu Z., Wang J., Liang J. Experimental measurement and analysis of the optical trapping force acting on a yeast cell with a lensed optical fiber probe. *Optics&Laser Technology* 2007; 39(3): 475-480. DOI: 10.1016/j.optlastec.2005.11.010
9. Liao G.-B., Chen Y.-Q., Bareil P.B., Sheng Y., Chiou A., Chang M.-S. Radiation pressure on a biconcave human Red Blood Cell and the resulting deformation in a pair of parallel optical traps. *J. Biophotonics* 2014; 7(10): 782-787. DOI: 10.1002/jbio.201300017
10. Roosen G., Imbert C. Optical levitation by means of two horizontal laser beams: a theoretical and experimental study. *Physics Letters A* 1976; 59(1): 6-8. DOI: 10.1016/0375-9601(76)90333-9
11. Ashkin A. Forces of a single-beam gradient laser trap on a dielectric sphere in the ray optics regime. *Biophys. J.* 1992; 61: 569-582. DOI: 10.1016/S0006-3495(92)81860-X
12. Gu M., Bao H., Gan X., Stokes N., Wu J. Tweezing and manipulating micro- and nanoparticles by optical non-linear endoscopy. *Light: Science & Applications* 2014; 3: 1-6. DOI: 10.1038/lsa.2014.7
13. Park B.J., Furst E.M. Effects of coating on the optical trapping efficiency of microspheres via geometrical optics approximation. *Langmuir* 2014; 30(37): 11055-11061. DOI: 10.1021/la502632h
14. Haghshenas-Jaryani M., Black B., Ghaffari S., Drake J., Bowling A., Mohanty S. Dynamics of microscopic objects in optical tweezers: experimental determination of underdamped regime and numerical simulation using multiscale analysis. *Nonlinear Dynamics* 2013; 76(2): 1013-1030. DOI: 10.1007/s11071-013-1185-0
15. Thalhammer G., Obmascher L., Ritsch-Marte M. Direct measurement of axial optical forces. *Optics Express* 2015; 23(5): 6112-6129. DOI: 10.1364/OE.23.006112
16. Lee K.S., Yoon S.Y., Lee K.H., Kim S.B., Sung H.J., Kim S.S. Radiation forces on a microsphere in an arbitrary refractive index profile. *J. Opt. Soc. Am. B.* 2012; 29(3): 407-414. DOI: 10.1364/JOSAB.29.000407
17. Callegari A., Mijalkov M., Gokoz A.B., Volpe G. Computational toolbox for optical tweezers in geometrical optics. *J. Opt. Soc. Am. B* 2015; 32(5): B11-B19. DOI: 10.1364/JOSAB.32.000B11
18. Kim S.B., Kim S.S. Radiation forces on spheres in loosely focused Gaussian beam: ray-optics regime. *J. Opt. Soc. Am. B* 2006; 23(5): 897-903. DOI: 10.1364/JOSAB.23.000897
19. Dutra R.S., Viana N.B., Maia Neto P.A., Nussenzveig H.M. Absolute calibration of forces in optical tweezers. *Phys. Rev. A.* 2014; 90: 013825-1 – 013825-13. DOI: 10.1103/PhysRevA.90.013825
20. Bashkatov A.N., Zhestkov D.M., Genina E.A., Tuchin V.V. Immersion clearing of human blood in the visible and near-infrared spectral regions. *Optics and Spectroscopy* 2005; Vol. 98(4): 638-646. DOI: 10.1134/1.1914906
21. Im K.-B., Lee D.-Y., Kim H.-I., Oh C.-H., Song S.-H., Kim P.-S. Calculation of optical trapping forces on micro-

spheres in the ray optics regime. J. Kor. Phys. Soc. 2002; 40(5): 930-933

■ **22.** Volpe Gior., Volpe Giov. Simulation of a Brownian particle in an optical trap. Am. J. Phys. 2013; 81(3): 224-230. DOI: 10.1119/1.4772632

■ **23.** Happel J., Brenner H. Low Reynolds number hydrodynamics. Springer Netherlands, 1983. DOI: 10.1007/978-94-009-8352-6

